Environ Sci Pollut Res (2017) 24:4882–4893
DOI 10.1007/s11356-016-8171-2

RESEARCH ARTICLE

The characteristics of steel slag and the effect of its application as a soil additive on the removal of nitrate from aqueous solution

Yang Liyun[1] · **Xu Ping**[1] · **Yang Maomao**[1] · **Bai Hao**[1]

Received: 19 July 2016 / Accepted: 28 November 2016 / Published online: 17 December 2016

Abstract This study examined the characteristics of nitrate removal from aqueous solution by steel slag and the feasibility of using steel slag as a soil additive to remove nitrate. Steel slag adsorbents were characterized by X-ray fluorescence (XRF), X-ray diffraction (XRD), scanning electron microscopy (SEM) and infrared spectrum (IR spectrum). Adsorption isotherms and kinetics were also analysed. Various parameters were measured in a series of batch experiments, including the sorbent dose, grain size of steel slag, reaction time, initial concentration of nitrate nitrogen, relationship between Al, Fe and Si ions leached from the steel slag and residual nitrate in the aqueous solution. The nitrate adsorbing capacity increased with increasing amounts of steel slag. In addition, decreasing the grain diameter of steel slag also enhanced the adsorption efficiency. Nitrate removal from the aqueous solution was primarily related to Al, Fe, Si and Mn leached from the steel slag. The experimental data conformed to second-order kinetics and the Freundlich isothermal adsorption equation, indicating that the adsorption of nitrate by steel slag is chemisorption under the action of monolayer adsorption. Finally, it was determined that using steel slag as a soil additive to remove nitrate is a feasible strategy.

Keywords Steel slag · Nitrate · Removal characteristics · Soil additives · Adsorption kinetics · Adsorption isotherm

Responsible editor: Philippe Garrigues

✉ Yang Liyun
Yangliyun@ustb.edu.cn

Xu Ping
wendy6393@163.com

Yang Maomao
15600928636@163.com

Bai Hao
baihao@metall.ustb.edu.cn

[1] Department of Ecological Science and Engineering, School of Metallurgical and Ecological Engineering, University of Science and Technology Beijing, Beijing 100083, China

Introduction

Recently, nitrate contamination of aqueous environments has become a serious global concern. The production activities and lifestyles of modern human populations (e.g., domestic sewage, wastes and excrement, chemical fertilizers, industrial sewage and wastewater irrigation) have resulted in the accumulation of nitrate at high concentrations on land and in water environments, posing a threat to human health and ecosystem stability (Feleke and Sakakibara 2002; Fewtrell 2004; Keränen et al. 2015; Wiesmann et al. 2007). Therefore, nitrate removal from water is critically important for both the environment and human health (Elmidaoui et al. 2001). Common methods for removing nitrate from water include biological denitrification, chemical reduction, reverse osmosis and adsorption (Bae et al. 2002; Li et al. 2010; Park et al. 2009; Schoeman and Steyn 2003; Tchobanoglous 1979). Adsorption is one of the most economical and efficient methods of nitrate removal due to its low initial cost, low energy requirements, ease of design and possibility of reusing adsorbents via regeneration. Consequently, adsorption has received considerable attention in recent years (Namasivayam et al. 2001). Although many different materials can be used as adsorbents to remove pollutants from water, the cost and availability of most cannot meet the demands of large-scale sewage treatment (Keränen et al. 2015; Mishra and Patel 2009; Mizuta et al. 2004; Öztürk and Bektaş 2004).

Consequently, there is a need to develop a practical and cost-effective adsorbent that can be used widely to remove nitrate from water. Low-cost alternatives based on mineral adsorbents and agricultural or industrial by-products have been studied for wastewater remediation (Pollard et al. 1992).

Steel slag, an industrial by-product, is generated annually in enormous quantities from steel manufacturing processes (Pollard et al. 1992). Slag consists mainly of calcium oxide, aluminium oxide, manganese oxide and iron oxide. These oxides in slag provide adsorption sites for anions. Due to its availability and advantageous composition as an adsorbent, various studies of the utilization of slag as an adsorbent for phosphate and heavy metals have been conducted (Barca et al. 2012; Kanel et al. 2006; Oh et al. 2012). When steel slag is used as a substrate in wetlands, the wetland system can effectively remove total nitrogen, nitrate and ammonia nitrogen (Xiong et al. 2011). As a substrate, steel slag reduces total nitrogen and ammonia nitrogen more efficiently compared with bamboo charcoal or limestone under the same wetland conditions (Lu et al. 2016). However, the nitrate adsorption characteristics of steel slag in water have not been thoroughly discussed.

In general, accumulated nitrate on land surfaces is absorbed by or infiltrates into the soil during run-off from rainfall events. Thus, soil plays an important role in reducing nitrate concentrations in run-off. As a highly porous medium, soil can adsorb and reduce some pollutants in run-off, including phosphate, sulphate and some organic components (Asano 1998; Yang et al. 2010; Yang et al. 2015). However, soil itself contains nitrate, which is readily soluble in water. Therefore, soil may actually increase nitrate concentrations in infiltrated water without denitrification by subsequent microorganisms (Cha et al. 2006), thereby aggravating pollution in groundwater. Steel slag can be added to the soil to enhance pollutant adsorption. The use of steel slag as a soil additive has been shown to improve phosphate and sulphate removal rates (Cha et al. 2006). The potential reduction of nitrate by steel slag as a soil additive has not been studied.

Therefore, this study first examined the removal mechanism of nitrate by steel slag using batch processing experiments, scanning electron microscopy (SEM) and X-ray diffraction (XRD). Second, the feasibility of using steel slag as a soil additive to remove nitrate was assessed.

Materials and methods

Collection and preparation of samples

Preparation of steel slag samples

The steel slag used in the experiments was collected from the Shijiazhuang Iron and Steel Plant in Shijiazhuang, Hebei Province, China. Samples of three different grain sizes (0.25, 0.85 and 4.00 mm) were obtained by crushing the slag with a jaw crusher and grinding with a planetary ball miller. The samples were washed with deionized water to remove particles and dried for 24 h at 100 °C before use in experiments. The chemical compositions and mineral phase constituents of the steel slag were analysed and determined by X-ray fluorescence (XRF) spectrographs (XRF-1800, Shimadzu, Japan) and XRD spectrograms (XRD-Rigaku MiniFlex 600, Japan), respectively.

Preparation of soil samples

Soil was sampled from the campus green land of the University Science and Technology Beijing, China. Soil samples were collected and air-dried for 1 week; then, plant roots were removed, and samples were crushed into equally distributed grains that were then ground in a ceramic mortar to obtain particles with a size of 0.25 mm. The soil sample pH was 8.1; organic matter content was 7.8 ± 0.526 mg/g; total nitrogen was 0.22 ± 0.017 mg/g, and total phosphorus was 0.47 ± 0.037 mg/g.

Preparation of nitrate solutions

Potassium nitrate (nitrate potash, SCRC, China) was used as the source of NO_3^--N. Before use in experiments, the potassium nitrate was dried at 105 °C for 2 h and then placed in an airtight drier. Nitrate solutions were prepared for follow-up experiments by dissolving various amounts of potassium nitrate in deionized water.

Leaching experiment

Several studies have noted that steel slag might release harmful metallic elements (Mann and Bavor 1993; Yan et al. 2000). Therefore, a leaching experiment was performed to verify the feasibility of using steel slag as an adsorbent by evaluating the potential release of harmful metallic elements. The experiment also measured the dynamics of Ca^{2+} and OH^- leached from different sizes of steel slag over different periods of time. The experiments were initiated by adding 40 g of steel slag sample of three different grain sizes to beakers containing 1 L of water. The beakers were then placed in an electrically heated thermostated water bath at 25 °C. The solutions were mechanically stirred at 125 rpm for 6, 12, 24, 48, 72, 120 and 168 h, respectively. The pH value and conductivity of the solutions filtered using mesoporous filter paper with a pore size of 30–50 μm were measured immediately after the reaction. The concentrations of various elements, including Ca, leached from the steel slag were measured simultaneously.

Removal of nitrate nitrogen by batch processing

The ability of steel slag to remove nitrate was studied using a series of batch processing experiments, and a mechanistic analysis was also performed. The main study parameters included grain size and the quantity of steel slag, reaction time and initial concentration of nitrate nitrogen. A preliminary analysis of the effects of pH on nitrate removal in the early stages of the experiment revealed that the effects of pH on adsorption were not obvious, possibly due to the use of a substantial amount of steel slag. Therefore, the pH of the nitrate nitrogen solution was controlled in this experiment.

A measured amount of steel slag was added to 1 L of nitrate solution and placed in an electrically heated thermostated water bath at 25 °C with mechanically stirring at 125 rpm for 24 h. To minimize the possibility of microbiological effects, 24 h was judged to be sufficient time to achieve steady state according to the Standard Test Method for 24-h Batch-Type Measurement of Contaminant Sorption by Soils and Sediments (D4646, 2003). Following the adsorption experiments, the samples were filtered to separate the supernatant liquid, and then, the pH, conductivity and Ca and Al concentrations were measured. The samples were centrifuged three times for 10 min at 4000 rpm and then dried in an oven at 100 °C for 12 h. Before and after the experiments, the mineral phase composition of the solid samples was determined by XRD spectrogram, and changes in surface appearance and the distribution of chemical elements were observed and analysed by SEM (JSM6480LV, Japan), X-ray energy-dispersive spectroscopy (EDS) (Noran System Six, USA) and infrared spectrum (IR spectrum) (Nicolet iS 5, Thermo Scientific, USA). The concentration of residual NO_3^--N was measured. The adsorption capacity (mg/g) and removal rate (%) were calculated using Eqs. (1) and (2), respectively.

$$NO_3^-\text{–N uptake (mg/g)} = \left(C_{\text{in}} - C_{fi}\right)V/M \quad (1)$$

$$NO_3^-\text{–N removed (\%)} = \left(C_{\text{in}} - C_{fi}\right)/C_{\text{in}} \times 100\% \quad (2)$$

In these equations, C_{in} and C_{fi} are the initial concentration (mg/L) and final concentration (mg/L) of NO_3^--N, respectively, M is the mass of the steel slag sample (g) and V is the volume of the solution.

Effect of sorbent dose

To study the effects of the steel slag sorbent dose on the adsorption of nitrate, steel slag samples of size 0.25 mm were mixed in different quantities (10, 20, 30, 40, 50 and 60 g) with 1 L of nitrate solution (100 mg N/L). The samples were stirred for 24 h and then filtered. The concentration of residual nitrate nitrogen, pH, conductivity and Ca and Al concentrations of the filtered solutions were measured.

Effect of grain size

To study the effects of steel slag grain size on the adsorption of nitrate, 50 g of steel slag samples of different grain sizes (0.25, 0.85 and 4.00 mm) was mixed with 1 L of nitrate solution (100 mg N/L). The samples were stirred for 24 h and then filtered. The concentration of residual nitrate nitrogen, pH, conductivity and Ca and Al concentrations of the filtered solutions were measured.

Effect of reaction time

To determine the equilibrium time of the reaction, beakers containing 50 g of steel slag samples (0.25 mm) in 1 L of nitrate solution (100 mg N/L) were placed in a thermostated water bath with a stirrer and stirred for various periods of time (6, 12, 24, 48, 72, 120 and 168 h). Each group of samples was filtered to measure the concentration of residual nitrate nitrogen, pH, conductivity and Ca and Al concentrations of the filtered solution.

Effect of initial concentration

In each group of experiments, 50 g of steel slag samples (0.25 mm) was added to 1 L of prepared solutions with different initial NO_3^--N concentrations (20, 40, 60, 80, 100 and 120 mg/L). The initial pH value of the solution was adjusted to 6.0 with HCl and NaOH (0.1 mol/L) before adding the steel slag. The samples were stirred for 24 h and then filtered before measuring the concentration of residual nitrate nitrogen, pH, conductivity and Ca, Al, Fe and Si concentrations of the filtered solutions.

Application of steel slag to soil

Mixed samples (a total of 50 g) of steel slag and soil with slag/soil mass ratios of 0, 5, 7 or 10%, corresponding to masses of slag and soil of 0, 2.5 g/47.5 g, 3.5 g/46.5 g and 5 g/45 g, respectively, were added to 1 L of synthetic solutions with a NO_3^--N concentration of 100 mg/L. After 24 h of mechanical stirring at 125 rpm at 25 °C, the samples were filtered, and then, the pH of the filtered solution and the concentration of residual NO_3^--N were measured.

Analytical methods

Chemical analysis

A multiparameter controller (Spectroquant NOVA 60, Merck KGaA, Germany) and a NO_3^--N detection reagent were used to determine the concentrations of nitrate nitrogen at equilibrium. Inductively coupled plasma atomic emission spectrometry (ICP-AES) (Optima 7000DV, PerkinElmer, USA) was

performed to analyse the elemental concentrations in the various solutions. Ca^{2+} ion concentrations were measured by EDTA titration. The pH values and electrical conductivity of the solutions were measured using an acidometer (PHS-3C, China) and conductivity meter (DDSJ-308F, China), respectively. All chemicals used were of analytical grade. In addition, all adsorption experiments were performed in triplicate, with data expressed as average values, and the standard deviation of the data in each group was calculated.

Adsorption model

Adsorption kinetics To investigate the NO_3^--N adsorption process, pseudo-first-order and pseudo-second-order kinetic models can be used, as proposed by Largergren (1898) and by Ho (1995), respectively. The first-order rate equation is the most commonly used kinetic equation applied to liquid-phase adsorption based on the solid adsorption capacity of Largergren (1898), whereas the second-order kinetic model is based on the assumption that the rate of adsorption is controlled by chemisorption mechanisms (Ho 1995). The kinetic models are as follows:

$$\log(Q_e - Q_t) = \log Q_e - K_1 t/2.303 \quad (3)$$

$$t/Q_t = 1/\left(K_2 Q_e^{\,2}\right) + t/Q_e \quad (4)$$

In Eqs. (3) and (4), Q_e and Q_t represent the adsorbing capacity of the reaction (mg/g) at equilibrium and time t, respectively. K_1 is the constant of the first-order rate of adsorption (1/h), and K_2 is the constant of the second-order rate of adsorption (g/(mg h)).

Adsorption isotherms To show the isothermal adsorption effects of NO_3^--N more clearly, several mathematical relationships were used to simulate the adsorption data. The Langmuir and Freundlich models are usually used to simulate isotherm data when the ion adsorption reaction occurs by monolayer adsorption. The Langmuir model assumes that the surface of the adsorbent is homogeneous, without any interaction between ions, and can fix metal ions (Langmuir 1916). The Freundlich model assumes that the surface of the adsorbent is heterogeneous and that ions adsorbed on the surface can mutually affect each other (Freundlich 1906). The linear equalities of the relevant models are as follows:

$$1/Q = 1/(K_L Q_m) \times 1/C_e + 1/Q_m \quad (5)$$

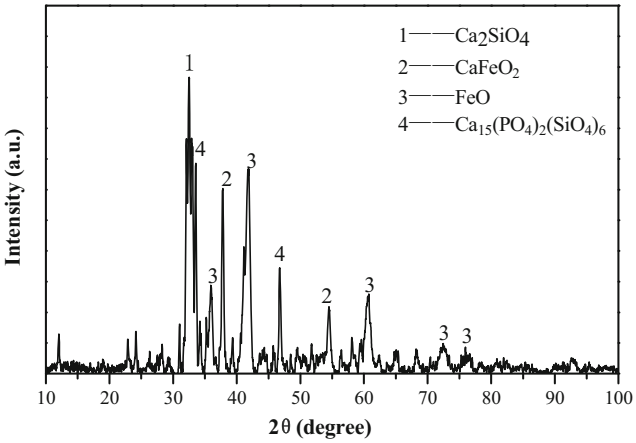

Fig. 1 Mineral phase constituents of steel slag analysed by XRD

In Eq. (5), Q refers to the equilibrium adsorption capacity (mg/g), namely the specific value of the dissolved mass adsorbed and the mass of adsorbent. In Eq. (1), for example, Q_m is the saturation adsorption capacity (mg/g), C_e refers to the equilibrium concentration of solute (mg/L) in the solution and K_L refers to the equilibrium constant (L/mg) related to the heat of adsorption:

$$\log Q = \log C_e/n + \log K_F \quad (6)$$

In Eq. (6), K_F is the Freundlich equilibrium constant ((mg/g) $(L/mg)^{1/n}$) and n (greater than 1) represents a model parameter related to temperature and porosity.

Results and discussion

Steel slag composition

XRF spectrometry revealed that the main chemical components of steel slag were CaO, SiO_2, FeO and Fe_2O_3, with small quantities of MnO, MgO and Al_2O_3 (Table 1). The percentage composition of basic oxides such as CaO and MgO exceeded 50%. According to Okada et al. (2003), the pore structure on the surface of Al_2O_3 can permit chemical adsorption of oxidative anions, as verified by other studies (Baker et al. 1998). The porous structure of SiO_2 can promote the adsorption of amine salt ions, whereas dissolved Ca^{2+} ions form precipitates with oxidized anions. Iron oxides in steel slag can also provide adsorption sites for anions (Fendorf et al. 1997). The main mineral phases of steel slag are Ca_2SiO_4, $CaFeO_2$, FeO and

Table 1 Chemical components of steel slag analysed by XRF

Chemical components	CaO	SiO_2	FeO	Fe_2O_3	MnO	MgO	P_2O_5	Al_2O_3	TiO_2
Percentage (%)	47.10	13.38	13.02	10.24	5.94	3.85	2.78	1.33	0.99

Table 2 Concentrations of toxic elements in leaching solutions of different grain size steel slag after 168 h (units: mg/L)

Measurement (168 h)	Cu	Zn	Pb	Cd	Cr	V	As
0.25-mm steel slag	≤0.002	≤0.002	≤0.03	≤0.002	≤0.003	≤0.003	≤0.03
0.85-mm steel slag	≤0.002	≤0.002	≤0.03	≤0.002	≤0.003	≤0.003	≤0.03
4.00-mm steel slag	≤0.002	≤0.002	≤0.03	≤0.002	≤0.003	≤0.003	≤0.03
Type III standard of surface water	1.0	1.0	0.05	0.005	0.05	0.05	0.05

$Ca_{15}(PO_4)_2(SiO_4)_6$ (Fig. 1). Among these, Ca_2SiO_4 and $CaFeO_2$ have particular gel properties.

Safety and ion-releasing properties of steel slag

The concentrations of toxic elements leached from the slag 24 h after the reaction of steel slag with different grain diameters (0.25, 0.85 and 4.00 mm) and their concentrations in type III standard surface water according to the National Environmental Quality Standards for Surface Water (GB3838-2002) are summarized in Table 2. The concentrations of toxic elements in the leachate from steel slag of three different grain sizes were below the detection limit of ICP-AES and far lower than type III standard values for surface water environmental quality, which suggests that there is a very low possibility that these elements are leached from steel slag. These results are identical to those of the Korean Standard Leaching Test (KSLT), which aims to explore the leaching properties of elements in steel slag (Oh et al. 2012). Therefore, as a wastewater adsorbent, steel slag will not produce secondary pollution and is safe for usage.

The pH values of the leachate solutions and the concentrations of Ca and heavy metals leached from the steel slag with a grain size of 0.25 mm after different reaction times are listed in Table 3. With increasing reaction time, the concentration of Ca and pH increased due to dissolution of CaO (Table 1) in the solution. The continuously increasing conductivity reflects the increasing leaching of ions from the slag with time throughout the 7-day reaction period. The kinetics of release indicated that 7 days is sufficient time for the ion concentrations to achieve equilibrium. Within this time period, the concentrations of toxic metals such as Cu, Zn, Pb and Cd were less than the detection limit of ICP-AES, which indicates that it is not likely that these metal elements leached from the slag.

Adsorption capacity of nitrate by steel slag

Effect of sorbent dose

Figure 2 illustrates the experimental results of removing NO_3^--N from 100 mg/L synthetic solutions with various steel slag sorbent doses. The more steel slag that was added, the more NO_3^--N was adsorbed because the increased specific surface area of the adsorbents enhanced the adsorbing capacity. The adsorbing capacity for NO_3^--N ranged from 0.22 to 0.64 mg/g (0.97 to 2.83 mg/g for nitrate). The maximum removal rate was 27.50% when the sorbent dose of steel slag reached 50 g. The addition of steel slag beyond 50 g did not further increase the removal rate. Conductivity, pH and Ca concentrations increased with increasing sorbent dosages. By contrast, with increasing sorbent dosages, the concentration of Al declined rapidly from 1.13 to 0.04 mg/L, and the final concentration was close to zero. At increasing sorbent dosages, more CaO in the steel slag dissolves in solution, and the concentrations of Ca^{2+} and OH^- increase accordingly (Barca et al. 2012). Therefore, our results indirectly prove that the elimination of NO_3^--N is not closely related to Ca and pH. By contrast, as the reaction proceeds, the concentration of Al decreases to zero, indicating that Al leached from the steel slag greatly influences the elimination of NO_3^--N.

Effect of grain size

The experiment above demonstrated that the maximum removal rate occurred at an input of 50 g of steel slag.

Table 3 Concentrations of elements leached from steel slag with a grain size of 0.25 mm at different times (units: mg/L)

Measurement	Conductivity (mS/cm)	pH	Ca	Cu	Zn	Pb	Cd	Cr	V	As
6 h	2.53	11.96	197.36	≤0.002	≤0.002	≤0.03	≤0.002	≤0.003	≤0.003	≤0.03
12 h	2.59	12.10	200.60	≤0.002	≤0.002	≤0.03	≤0.002	≤0.003	≤0.003	≤0.03
24 h	2.61	12.19	202.02	≤0.002	≤0.002	≤0.03	≤0.002	≤0.003	≤0.003	≤0.03
48 h	2.64	12.26	224.52	≤0.002	≤0.002	≤0.03	≤0.002	≤0.003	≤0.003	≤0.03
72 h	4.67	12.28	454.92	≤0.002	≤0.002	≤0.03	≤0.002	≤0.003	≤0.003	≤0.03
120 h	6.18	12.61	642.48	≤0.002	≤0.002	≤0.03	≤0.002	≤0.003	≤0.003	≤0.03
168 h	6.32	12.75	644.15	≤0.002	≤0.002	≤0.03	≤0.002	≤0.003	≤0.003	≤0.03

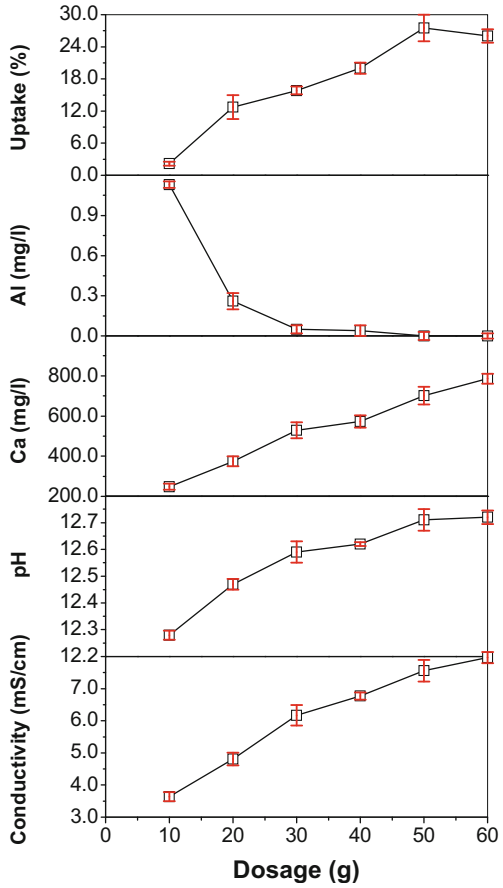

Fig. 2 NO_3^--N adsorption properties of steel slag samples, pH value and concentrations of Ca and Al in solution as a function of different sorbent doses (grain size of 0.25 mm, initial NO_3^--N concentration of 100 mg/L, reaction time of 24 h and initial pH without sorbent of 6)

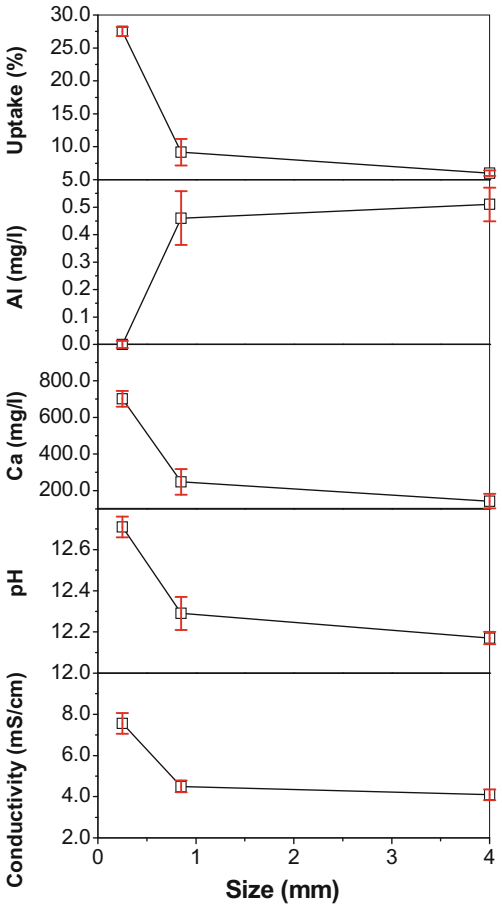

Fig. 3 NO_3^--N adsorption properties of steel slag samples, pH values and concentrations of Ca and Al in solutions with different grain sizes (the sorbent dose was 50 g/L, the initial NO_3^--N concentration was 100 mg/L, the reaction time was 24 h, and the initial pH without sorbent was 6)

Therefore, a second experiment was performed in which 50 g of steel slag of various particle sizes was added to remove NO_3^--N. The results of this experiment are shown in Fig. 3. As the grain size of the steel slag increased, the NO_3^--N adsorbing capacity decreased, ranging from 0.12 to 0.55 mg/g (0.53 to 2.44 mg/g for nitrate). The adsorption of NO_3^--N was greatest in steel slag samples with a grain size of 0.25 mm because the smaller sized particles increase the specific surface area. With increasing grain size, the variation trends of conductivity, pH and Ca concentration were opposite of those of the NO_3^--N concentration, whereas the trends of Al and NO_3^--N concentrations were similar.

Effect of reaction time

The experiment above demonstrated that steel slag samples with a grain size of 0.25 mm exhibited the greatest adsorption. As shown in Fig. 4, the NO_3^--N adsorbing capacity increased with time in synthetic solutions containing steel slag samples with a grain size of 0.25 mm. The amount of NO_3^--N adsorbed rapidly increased for the first 24 h but increased slowly or even decreased at longer reaction times. The adsorption capacity of NO_3^--N ranged from 0.28 to 0.58 mg/g (1.24 to 2.57 mg/g for nitrate). Under normal conditions, as the reaction time increased, the adsorption effect gradually stabilized (Ćurković et al. 2001; Ho et al. 2004). The conductivity, pH and Ca concentration increased dramatically during the first 24 h and reached a plateau at longer reaction times. However, the concentration of Al decreased rapidly within the first 12 h, and little Al remained in solution after 24 h. The leaching rate of Al_2O_3 from steel slag was greater than the rate of elimination of NO_3^--N in solution within the first 12 h. Therefore, during this time, the concentration of Al in the solution increased. As the reaction proceeded, the Al that had leached into the solution was eliminated, and the reaction was complete when the concentration of Al reached zero.

Effect of the initial concentration

Based on the results of the three experiments described above, the optimum parameters for steel slag are a sorbent dose of 50 g, grain size of 0.25 mm and reaction time of 24 h. To

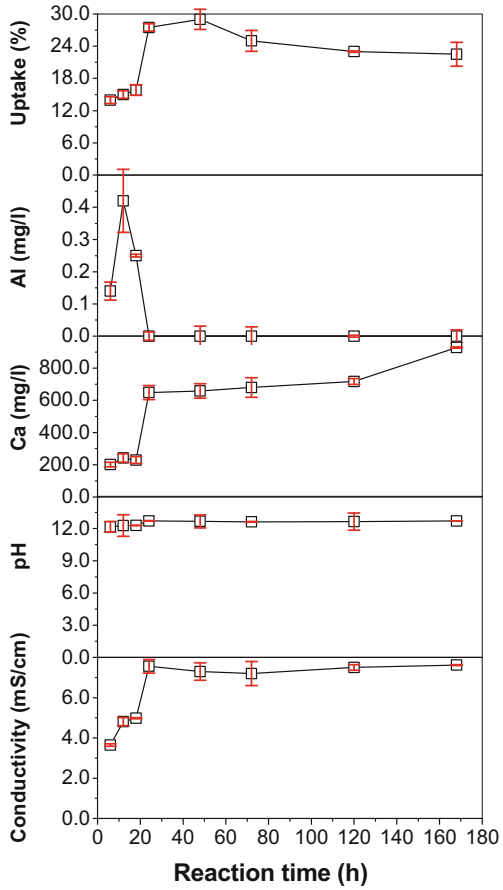

Fig. 4 NO_3^--N adsorption properties of 0.25-mm steel slag samples and changes in pH and concentrations of Ca and Al in solution with increasing reaction time (the grain size was 0.25 mm, the initial NO_3^--N concentration was 100 mg/L, the sorbent dose was 50 g/L, and the initial pH without sorbent was 6)

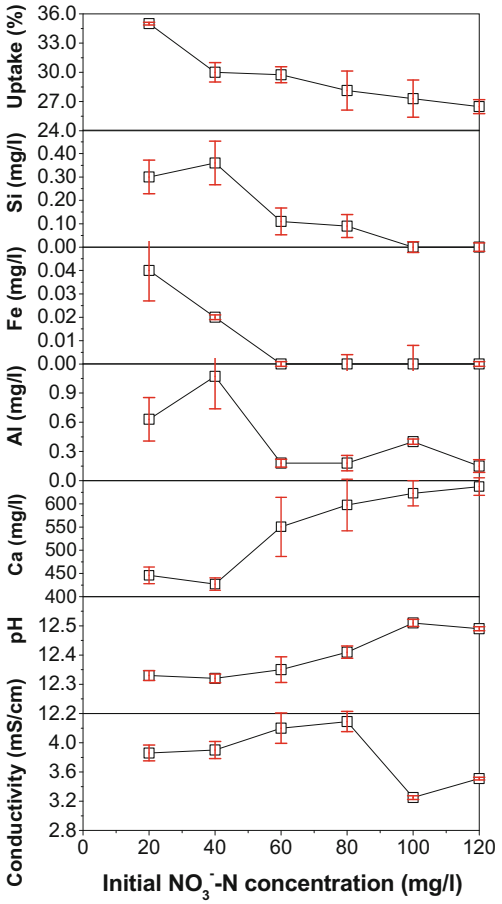

Fig. 5 NO_3^--N adsorption properties of steel slag samples and changes in pH and concentrations of Ca, Al, Si and Fe in solution under the optimum compounding ratio (the grain size was 0.25 mm, the sorbent dose was 50 g/L, the reaction time was 24 h, and the initial pH without sorbent was 6)

further examine these parameters, these optimum conditions were used in an adsorption experiment with different initial concentrations of NO_3^--N (Fig. 5). The initial concentration of NO_3^--N has a huge influence on removal rates. The adsorbing capacity of the steel slag dramatically increased with increasing initial NO_3^--N concentration. The adsorbing capacity ranged from 0.14 to 0.64 mg/g (0.62 to 2.83 mg/g for nitrate), and the largest adsorption capacity was observed when the concentration of NO_3^--N was 120 mg/L. These results demonstrate that NO_3^--N was not completely eliminated, similar to results reported by Barca et al. (2012), who used steel slag to remove phosphate from wastewater. As the nitrate concentration increased, the concentration of Al decreased, as shown in previous experiments, and the concentrations of Fe and Si also decreased. The concentration of Fe in the solution decreased to zero when the initial concentration of NO_3^--N was 60 mg/L, but Si and Al were still present. Thus, Fe dissolved from steel slag was completely removed at this NO_3^--N concentration, whereas Si could not be eliminated at an initial NO_3^--N concentration of less than 100 mg/L. Similar to Al, Si remained in solution over the full range of initial concentrations of NO_3^--N because Fe in solution reacts more readily with elements involved in the elimination of NO_3^--N. When Fe was depleted, Si replaced Fe, and both were eventually depleted. The reaction was not complete, as some Al remained in solution. Thus, these three elements have a huge influence on the elimination of nitrate. Steel slag also contains some secondary, positively charged aluminium silicate, calcium silicate and silicate, which can adsorb nitrate by ion exchange or by forming ion pairs. Moreover, steel slag containing iron oxide, aluminium oxides, etc., generates flocculating constituents in alkaline conditions, leading to nitrate coprecipitation by the sweep flocculation effect.

Morphology and structural composition of steel slag

The microtopography of the steel slag was analysed using SEM before and after the experiments. The surface of the slag was uneven, with debris (Fig. 6a, b), and after the adsorption experiment, many visible deposits appeared on the surface (Fig. 6c, d). Analysis of these deposits by EDS revealed that

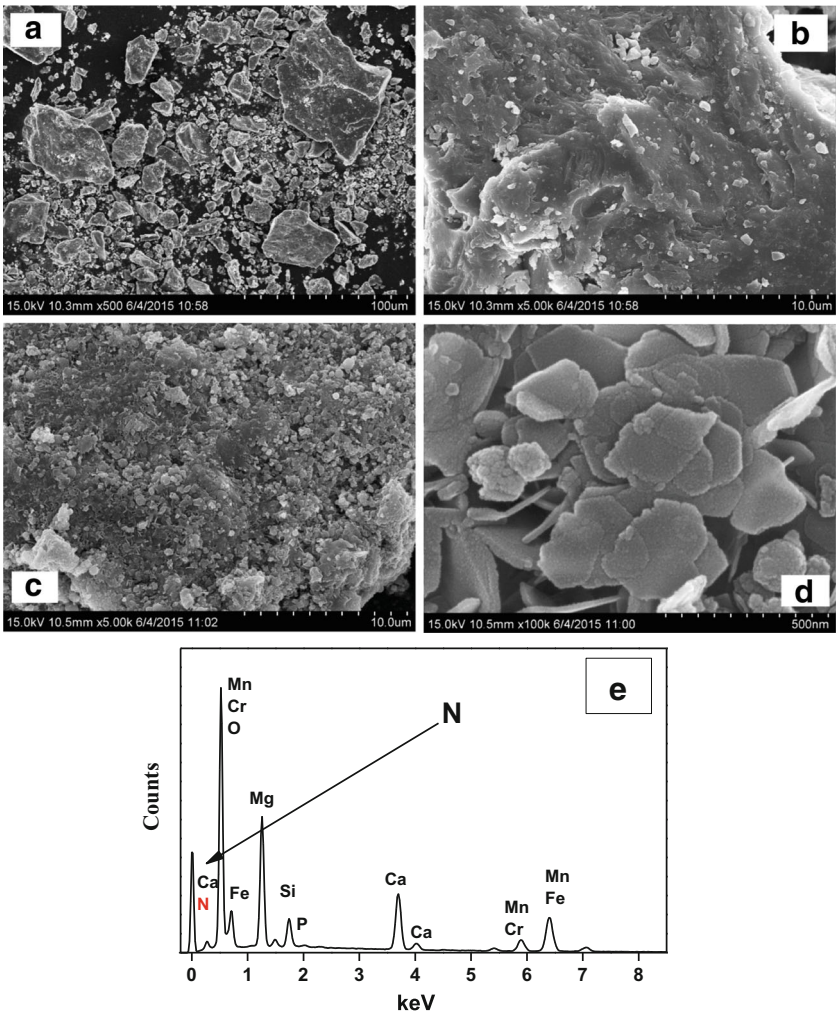

Fig. 6 SEM images of steel slag surfaces and results of EDS analysis: **a**, **b** SEM image before elimination of NO_3^--N and **c**, **d** SEM image after elimination of NO_3^--N. **e** Chemical result of EDS analysis after elimination of NO_3^--N (magnification **a** ×500, **b** ×5000, **c** ×5000 and **d** ×100k)

N was present (Fig. 6e). Although N is a light element and difficult to accurately determine (Keränen et al. 2013), we found the presence of nitrogen on the surface of the steel slag at multiple detection points by EDS. EDS analysis can also be used to determine possible mineral phases formed by NO_3^--N and other elements (Matera et al. 2003). The batch processing experiments described above demonstrated that Al, Fe and Si in steel slag all participated in NO_3^--N elimination. Thus, the SEM images and the results of the EDS analyses support the experimental results described above.

Nitrate is a planar triangle, and its structure is 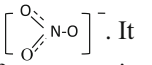 . It has two very characteristic active fundamental frequency vibrations. The strong and broad absorption band of 1400–1370 cm^{-1} belongs to the N–O stretching vibration, and the absorption spectrum of 850–800 cm^{-1} is of moderate

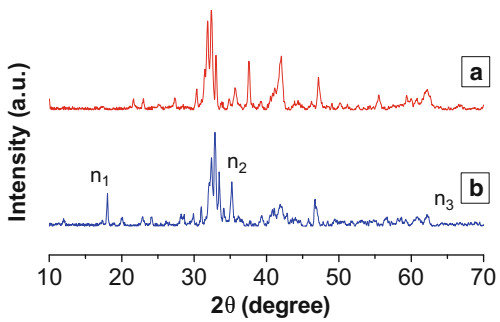

Fig. 7 XRD spectra of steel slag: **a** before elimination of NO_3^--N and **b** phase identification after elimination of NO_3^--N: MnO_2 (n_1), $MnCr_2O_4$ (n_2) and Mn_3N_2 (n_3)

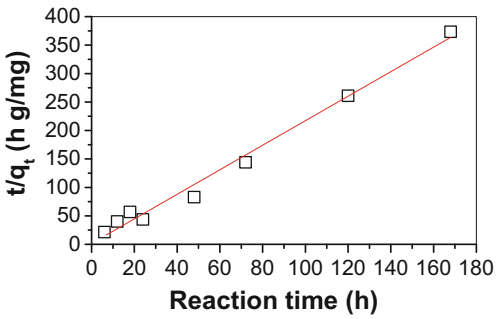

Fig. 8 Second-order kinetic linear graph of steel slag adsorption of NO_3^--N

Table 4 Parameters and correlation coefficients of the two kinetic models

Adsorbate	First-order kinetic model			Second-order kinetic model		
	Q_e (mg/g)	K_1 (1/h)	R^2	Q_e (mg/g)	K_2 (g/(mg h))	R^2
NO_3^--N	0.50	0.0976	0.8452	0.46	2.8185	0.9895

intensity. In this experiment, two obvious characteristic peaks, 1384.15 and 843.74 cm^{-1}, were observed after the absorption of nitrate, which showed that the surface of the steel slag contained nitric acid groups. The peaks of slag after adsorption appeared at 3644.02, 3554.63 and 915.99 cm^{-1}, respectively, characteristic peaks of aluminium hydroxide. These results are consistent with the presence of aluminium hydroxide on the surface of the slag after adsorption.

XRD spectral analyses were conducted to assess changes in mineral phases before and after the use of steel slag to remove NO_3^--N. After the adsorption experiment, there was a significant change in the XRD steel slag spectrum peaks. The new peaks were different mineral phases formed by manganese (Fig. 7). In addition to manganese (MnO_2) and manganochromite ($MnCr_2O_4$), there was a small amount of manganese nitride (Mn_3N_2). These results further demonstrate that steel slag can adsorb NO_3^--N. Moreover, this type of effect shares some features with manganese in steel slag. There has been no previous research examining the relationships between Mn and NO_3^--N.

Model analysis

Adsorption kinetics

The model parameters simulated from the experimental data above are presented in Table 4. The correlation coefficient of the second-order kinetic model (R^2 = 0.9895) is much greater than that of the first-order kinetic model (R^2 = 0.8452), and the second-order kinetic model agrees well with the experimental data (Fig. 8), indicating that the second-order rate equation can simulate the actual adsorption process of NO_3^--N quite well. The adsorption rate of NO_3^--N was 2.819 g/(mg h). These results also illustrate that chemical sorption involves valence forces through sharing or exchange of electrons between the adsorbent and adsorbate.

The adsorption of NO_3^--N was related to the concentration of dissolved Al, Fe and Si in the steel slag adsorption experiments. EDS analysis detected the presence of nitrogen on the surface of the steel slag after elimination of nitrate. The IR spectrum demonstrated that the surface of the steel slag after adsorption obviously contained nitric acid groups. In addition, XRD analysis showed that Mn and NO_3^--N formed a new mineral phase as a result of the adsorption reaction. The adsorption process simulated by the kinetic adsorption model demonstrated that the adsorption of nitrate by the steel slag was chemical adsorption. Fe, Al and other metal ions in the aqueous solution formed hydroxides and hydrous metal oxides on the surface of steel slag according to the degree of coordination of water (Fig. 9). Consequently, a number of –OH groups were present on the mineral interface, resulting in the formation of a hydroxylated mineral interface. NO_3^- was adsorbed through ligand exchange of metal ions. Surface coordination reactions often lead to an increase in pH, which can be explained by Eq. (7):

$$Al/Fe{-}OH + NO_3^- = Al/Fe{-}NO_3^- + OH^- \quad (7)$$

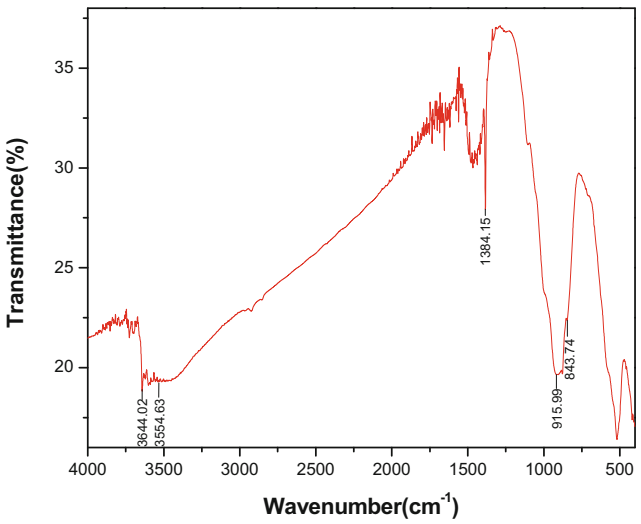

Fig. 9 IR spectrum of steel slag after elimination of NO_3^--N

Adsorption isotherm

The Langmuir adsorption isotherm and the Freundlich adsorption isotherm were drawn based on the experimental data above (Fig. 10), and the detailed parameters are shown in Table 5. The comparison of the correlation equilibrium coefficients in the two models showed that the Freundlich model appears to simulate our experimental data better than the Langmuir model. According to Samarghandi et al. (2010), the adsorption effect is good when the value of n calculated from the intercept of the fitted lines ranges between 1 and 10, indicating that slag is conducive to adsorption of NO_3^--N. This result also implies that the NO_3^--N is adsorbed through monolayer adsorption with heterogeneous surfaces in the adsorbent and that the adsorbed ions mutually interact.

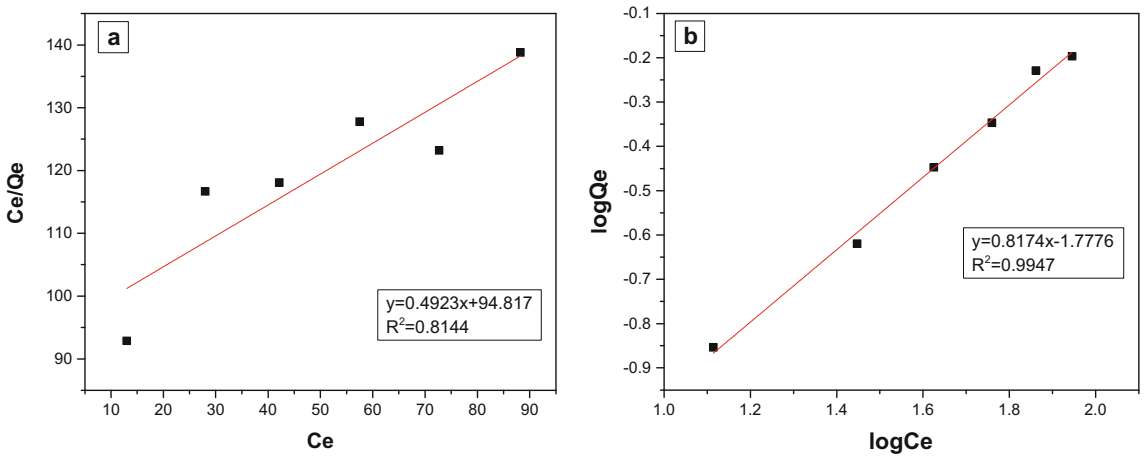

Fig. 10 Adsorption isotherm of NO_3^--N: **a** Langmuir model and **b** Freundlich model

Analysis of the adsorption kinetic model showed that the steel slag chemically adsorbed NO_3^--N. Compared with physical adsorption, a chemically adsorbed layer can only be a monolayer, consistent with the analysis of the adsorption isotherm model. Monolayer adsorption implies that the adsorption sites on the surface of the adsorbent can adsorb a maximum of one layer of molecules. In addition, a comparison of the adsorption capacity (mg/g) and other experimental conditions of different unmodified sorbents for nitrate removal is shown in Table 6. Compared with other minerals (e.g., agricultural or industrial by-products), in aqueous solution, steel slag has intermediate nitrate removal capabilities.

Feasibility analysis of applying steel slag to soil

The concentrations of residual NO_3^--N released from the mixed samples revealed that the concentrations of NO_3^--N were higher than the initial concentration (100 mg/L) in solutions with 0, 5 and 7% steel slag (Fig. 11a), indicating that the concentration of NO_3^--N released by the soil was higher than the amount absorbed by the steel slag. Mixed samples with 10% steel slag had a greater adsorption effect on the synthetic solution, reducing the concentration of residual NO_3^--N below that of the initial concentration, with a removal rate of 2.33%. In addition, the soils used in the experiment were all alkaline, and the steel slag was strongly alkaline. Thus, when the two were mixed, disposed and compounded into solution, the pH of the final solution was greater than 11 (Fig. 11b). This may have affected the growth of oxyphytes to some extent, but suitable vegetation could be chosen for alkaline soil. Moreover, steel slag can improve acidic soil (Gu et al. 2011; Qiu et al. 2012; Mäkelä et al. 2012); thus, applying steel slag to soil is conducive to eliminating NO_3^--N in sewage flowing out over green belt soils.

Table 5 Langmuir and Freundlich parameters and correlation coefficients of NO_3^--N adsorption

Adsorbate	Langmuir constant			Freundlich constant		
	Q_m (mg/g)	K_L (L/mg)	R^2	K_F ((mg/g) $(L/mg)^{1/n}$)	n	R^2
NO_3^--N	2.031	0.005	0.814	0.017	1.223	0.995

Table 6 Comparative evaluation of adsorption capacity and other experimental conditions of different unmodified sorbents for nitrate removal

Adsorbent	Experimental conditions	Amount adsorbed	References
Hydroxyapatite	pH 6.0 Concentration range 100 mg/L Temperature 50 °C	21 mg/g	Islam et al. (2010)
Halloysite	pH 5.4 Concentration 100 mg/L Room Temperature	0.54 mg/g	Xi et al. (2010)
Untreated coconut granular activated carbon	pH 5.5 Concentration range 5–200 mg/L Temperature 25 °C	1.7 mg/g	Bhatnagar et al. (2008)
Bamboo powder charcoal	pH n.a. Concentration range 0–10 mg/L Temperature 10 °C	1.25 mg/g	Mizuta et al. (2004)
Nano-alumina	pH 4.4 Concentration range 1–100 mg/L Temperature 25 °C	4.0 mg/g	Bhatnagar et al. (2010)
Steel slag	pH 6.0 Concentration range 89–531 mg/L Temperature 25 °C	2.83 mg/g	Present study

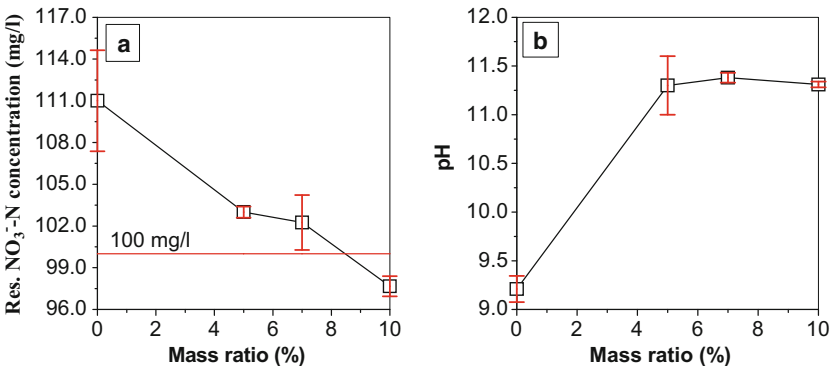

Fig. 11 **a** Adsorption effect on NO_3^--N. **b** pH of the final solution of mixed samples with different proportions of steel slag and soil

Conclusions

In assessing whether steel slag could be used as an adsorbent for eliminating nitrate in aqueous solutions, leaching experiments demonstrated that the concentrations of toxic elements of steel slag were below the detection limit of ICP-AES and far lower than the type III standard value of surface water environmental quality, which implies that steel slag will not cause secondary pollution. The subsequent series of batch processing experiments verified that steel slag can eliminate nitrate from aqueous solutions. The main experimental parameters affecting the elimination of nitrate are the input quantity and grain size of the steel slag, the reaction time and the initial concentration of nitrate. The large amounts of Al, Fe and Si in steel slag, which can adsorb nitrate, have a distinct proportional relationship with the elimination of NO_3^--N. In addition, various mineral phases of Mn, such as manganese nitrate, appeared during the experiment. The equilibrium data for the adsorption of NO_3^--N were consistent with the expression of second-order kinetics. The equation of the Freundlich isothermal adsorption model indicated that the NO_3^--N adsorption effect of the steel slag is chemisorption, the surface of the adsorbent is heterogeneous and reactions occur among the adsorbed ions. The silicate, iron and aluminium oxides present in steel slag were the principal materials generated by the removal reaction. In addition, it is feasible to apply steel slag to soil to remove NO_3^--N. In this respect, steel slag holds promise for surface sewage run-off and can be used as a soil additive and inexpensive adsorption material to eliminate NO_3^--N in water to reduce aqueous environmental pollution.

Acknowledgements Financial support for this study was provided by the 10-Year Evaluation Project of the People's Republic of China Ministry of Environmental Protection (STSN-06). We are very grateful to the referees and the editors for their helpful suggestions.

References

Asano T (1998) Wastewater reclamation and reuse. Wastewater reclamation and reuse. Technomic Pub, Chicago

Bae BU, Jung YH, Han WW, Shin HS (2002) Improved brine recycling during nitrate removal using ion exchange. Water Res 36:3330–3340

Baker MJ, Blowes DW, Ptacek CJ (1998) Laboratory development of permeable reactive mixtures for the removal of phosphorus from onsite wastewater disposal systems. Environ Sci Technol 32: 2308–2316

Barca C, Gérente C, Meyer D, Chazarenc F, Andrès Y (2012) Phosphate removal from synthetic and real wastewater using steel slags produced in europe. Water Res 46:2376–2384

Bhatnagar A, Ji M, Choi YH, Jung W, Lee SH, Kim SJ, Lee G, Suk H, Kim HS, Min B, Kim SH, Jeon BH, Kang JW (2008) Removal of nitrate from water by adsorption onto zinc chloride treated activated carbon. Sep Sci Technol 43(4):886–907

Bhatnagar A, Kumar E, Sillanpää M (2010) Nitrate removal from water by nano-alumina: characterization and sorption studies. Chem Eng J 163(3):317–323

Cha W, Kim J, Choi H (2006) Evaluation of steel slag for organic and inorganic removals in soil aquifer treatment. Water Res 40: 1034–1042

Ćurković L, Cerjan-Stefanović Š, Rastovean-Mioe A (2001) Batch Pb^{2+} and Cu^{2+} removal by electric furnace slag. Water Res 35:3436–3440

Elmidaoui A, Elhannouni F, Sahli MM, Chay L, Elabbassi H, Hafsi M et al (2001) Pollution of nitrate in Moroccan ground water: removal by electrodialysis. Desalination 136:325–332

Feleke Z, Sakakibara Y (2002) A bio-electrochemical reactor coupled with adsorber for the removal of nitrate and inhibitory pesticide. Water Res 36:3092–3102

Fendorf S, Eick MJ, Grossl P, Sparks DL (1997) Arsenate and chromate retention mechanisms on goethite. 1. Surface structure. Environ Sci Technol 31:315–320

Fewtrell L (2004) Drinking-water nitrate, methemoglobinemia, and global burden of disease: a discussion. Environ Health Perspect 112: 1371–1374

Freundlich H (1906) Über die adsorption in lösungen, zeitschrift für physikalische chemie. Jamchemsoc 62(5):121–125

Gu HH, Qiu H, Tian T, Zhan SS, Chaney RL, Wang SZ (2011) Mitigation effects of silicon rich amendments on heavy metal accumulation in rice (*Oryza sativa* l.) planted on multi-metal contaminated acidic soil. Chemosphere 83:1234–1240

Ho YS (1995) Adsorption of heavy metals from waste streams by peat. University of Birmingham, Birmingham

Ho YS, Chiu WT, Hsu CS, Huang CT (2004) Sorption of lead ions from aqueous solution using tree fern as a sorbent. Hydrometallurgy 73: 55–61

Islam M, Mishra PC, Patel R (2010) Physicochemical characterization of hydroxyapatite and its application towards removal of nitrate from water. J Environ Manag 91(9):1883–1891

Kanel SR, Choi H, Kim JY, Vigneswaran S, Wang GS (2006) Removal of arsenic (iii) from groundwater using low-cost industrial by-products—blast furnace slag. Water Qual Res J Can 41(2):130–139

Keränen A, Leiviskä T, Gao BY, Hormi O, Tanskanen J (2013) Preparation of novel anion exchangers from pine sawdust and bark, spruce bark, birch bark and peat for the removal of nitrate. Chem Eng Sci 98:59–68

Keränen A, Leiviskä T, Hormi O, Tanskanen J (2015) Removal of nitrate by modified pine sawdust: effects of temperature and co-existing anions. J Environ Manag 147:46–54

Langmuir I (1916) The constitution and fundamental properties of solids and liquids. Part i Solids J Am Chem Soc 38:2221–2295

Largergren S (1898) Zur theorie der sogenannten adsorption geloster stoffe. Kungliga Svenska Vetenskapsakademiens Handlingar 24: 1–39

Li J, Li Y, Meng Q (2010) Removal of nitrate by zero-valent iron and pillared bentonite. J Hazard Mater 174:188–193

Lu S, Zhang X, Wang J, Pei L (2016) Impacts of different media on constructed wetlands for rural household sewage treatment. J Clean Prod 127:325–330

Mäkelä M, Watkins G, Pöykiö R, Nurmesniemi H, Dahl O (2012) Utilization of steel, pulp and paper industry solid residues in forest soil amendment: relevant physicochemical properties and heavy metal availability. J Hazard Mater 207:21–27

Mann RA, Bavor HJ (1993) Phosphorus removal in constructed wetlands using gravel and industrial waste substrata. Water Sci Technol J Int Assoc Water Poll Res Control 27(1):107–113

Matera V, Le Hecho I, Laboudigue A, Thomas P, Tellier S, Astruc M (2003) A methodological approach for the identification of arsenic bearing phases in polluted soils. Environ Pollut 126:51–64

Mishra P, Patel R (2009) Use of agricultural waste for the removal of nitrate-nitrogen from aqueous medium. J Environ Manag 90: 519–522

Mizuta K, Matsumoto T, Hatate Y, Nishihara K, Nakanishi T (2004) Removal of nitrate-nitrogen from drinking water using bamboo powder charcoal. Bioresour Technol 95:255–257

Namasivayam C, Radhika R, Suba S (2001) Uptake of dyes by a promising locally available agricultural solid waste: coir pith. Waste Manag 21:381–387

Oh C, Rhee S, Oh M, Park J (2012) Removal characteristics of as (iii) and as (v) from acidic aqueous solution by steel making slag. J Hazard Mater 213:147–155

Okada K, Temuujin J, Kameshima Y, MacKenzie KJ (2003) Simultaneous uptake of ammonium and phosphate ions by composites of γ-alumina/potassium aluminosilicate gel. Mater Res Bull 38: 749–756

Öztürk N, Bektaş TE (2004) Nitrate removal from aqueous solution by adsorption onto various materials. J Hazard Mater 112:155–162

Park J, Craggs R, Sukias J (2009) Removal of nitrate and phosphorus from hydroponic wastewater using a hybrid denitrification filter (hdf). Bioresour Technol 100:3175–3179

Pollard S, Fowler G, Sollars C, Perry R (1992) Low-cost adsorbents for waste and wastewater treatment: a review. Sci Total Environ 116: 31–52

Qiu H, Gu H, He EK, Wang SZ, Qiu RL (2012) Attenuation of metal bioavailability in acidic multi-metal contaminated soil treated with fly ash and steel slag. Pedosphere 22:544–553

Samarghandi MR, Hadi M, Moayedi S, Askari FB (2010) Two-parameter isotherms of methyl orange sorption by pinecone derived activated carbon. Iran J Environ Health Sci Eng 6(4):285–294

Schoeman J, Steyn A (2003) Nitrate removal with reverse osmosis in a rural area in South Africa. Desalination 155:15–26

Tchobanoglous MEI (1979) Wastewater engineering: treatment, disposal, re-use, 2nd edn 07 A MET. McGraw-Hill Book Company, New York, p. 938

Wiesmann U, Choi IS, Dombrowski EM (2007) Fundamentals of biological wastewater treatment. John Wiley & Sons, Hoboken

Xi YF, Mallavarapu M, Naidu R (2010) Adsorption of the herbicide 2,4-D on organo-palygorskite. Appl Clay Sci 49(3):255–261

Xiong J, Guo G, Mahmood Q, Yue M (2011) Nitrogen removal from secondary effluent by using integrated constructed wetland system. Ecol Eng 37:659–662

Yan J, Moreno L, Neretnieks I (2000) The long-term acid neutralizing capacity of steel slag. Waste Manag 20:217–223

Yang H, McCoy EL, Grewal PS, Dick WA (2010) Dissolved nutrients and atrazine removal by column-scale monophasic and biphasic rain garden model systems. Chemosphere 80:929–934

Yang L, Zhang L, Li Y, Wu S (2015) Water-related ecosystem services provided by urban green space: a case study in Yixing city (China). Landsc Urban Plan 136:40–51